

# Machine learning approaches to seismic event classification in the Ostrava region

Marek Pecha<sup>1,4</sup>, Michael Skotnica<sup>1</sup>, Jana Rušajová<sup>1</sup>, Bohdan Rieznikov<sup>1,2</sup>,  
Vít Wandrol<sup>1,3</sup>, Markéta Rösnerová<sup>1</sup>, Jaromír Knejzlík<sup>1</sup>

<sup>1</sup> Institute of Geonics of the Czech Academy of Sciences, Ostrava, Czechia

<sup>2</sup> VŠB-Technical University of Ostrava, Czechia

<sup>3</sup> Brno University of Technology, Czechia

<sup>4</sup> Ullmanna, s.r.o., Opava, Czechia

## Abstract

The northeastern region of the Czech Republic is among the most seismically active areas in the country. The most frequent seismic events are mining-induced since there used to be strong mining activity in the past. However, natural tectonic events may also occur. In addition, seismic stations often record explosions in quarries in the region. Despite the cessation of mining activities, mine-induced seismic events still occur. Therefore, a rapid differentiation between tectonic and anthropogenic events is still important.

The region is currently monitored by the OKC seismic station in Ostrava-Krásné Pole built in 1983 which is a part of the Czech Regional Seismic Network. The station has been providing digital continuous waveform data at 100 Hz since 2007. In the years 1992–2002, the region was co-monitored by the Seismic Polygon Frenštát (SPF) which consisted of five seismic stations using a triggered STA/LTA system.

In this study, we apply and compare machine learning methods to the SPF dataset, which contains labeled records of tectonic and mining-induced events. For binary classification, a Long Short-Term Memory recurrent neural network and XGBoost achieved an F1-score of 0.94 – 0.95, demonstrating the potential of modern machine learning techniques for rapid event characterization.

## 1 Introduction

The northeastern region of the Czech Republic (Jeseníky Mountains, Opava Region, Upper Morava Valley) is one of our most seismically active areas in the country. In addition to tremors caused by coal mining, natural earthquakes also occur here. These are mostly very weak earthquakes with a magnitude of less than 0 and are only recorded by instruments. Occasionally, stronger earthquakes occur that are felt by people (e.g., Jeseníky Mountains in 1935, 1986, and 2012, or Opavsko in 1931, 1936, and a swarm in 1993). Between 1992 and 2002, the area was monitored by the Frenštát Seismic Polygon (SPF). During the entire period, the SPF recorded approximately 17,384 events, mostly induced seismic events related to mining in the OKR and Poland, a total of 14,144, followed by 2,516 natural earthquakes. Another type of phenomenon was quarry blast. There were 639 such events recorded. In addition, 85 other phenomena were not classified. There were 5,841 registered induced seismic events from OKR, with varying energy classes. There were 195 events with energy E+02 J, 3,586 with energy E+03J, 1,852

with energy E+04J, 182 with energy E+05J, 23 with energy E+06J, and 3 with energy E+07J. SPF registration was in trigonometric mode in the STA/LTA algorithm.

Since approximately 2010, IGN stations have switched to continuous recording with a sampling frequency of 100 Hz, which has resulted in a huge increase of the amount of data processed. Therefore, it is necessary to test machine learning methods for classifying induced seismic events in this area, as they can occur even after mining has ceased (mine flooding, etc.) and to quickly distinguish them from natural tectonic earthquakes.

In this study, we apply machine learning methods trained on the data from SPF to classify seismic events into two categories:

- Mining-induced seismic events,
- Natural tectonic seismic events.

## 2 Locality

Studied locality of Silesia and Northeast Moravia can be characterized by low natural seismic activity based on 30 years of seismological observations realized in the territory (see [PP22]). There are several seismically active areas, some of them are characterized even by occurring of seismic swarms (e.g. Opava in 1931 and Hradec nad Moravic  in 1993). The strongest earthquake instrumentally recorded at the locality occurred in 2017 near the Hlu  n town with local magnitude 3.5 (see [vZ18]). Nevertheless, stronger historical earthquakes with intensities up to  $Io=7$  are documented at the locality (e.g. Ostrava in 1786  $Io=7$ ; Bohum  n 1259  $Io=6$ ; Opava 1931  $Io=6$ ; see [D<sup>+</sup>97]) and Figure 1). Mining activities connected with underground exploitation of hard coal from Czech and Polish mines at the territory of the Upper Silesian Coal Basin (USCB) represent another important source of seismic activity in the region. It can be seen from Figure 1, that the strongest natural earthquakes (2017, 1786, 1259) are located close to mining claims in the Czech part of USCB. Thus, it could be expected that both types of seismic events, natural and mining induced (induced by mining or by flooding of closed parts of mines), could originate at the same locality. Therefore, investigation and recommendation of suitable discrimination techniques for determination of event s origin should be useful for future seismic observations at the territory.

For the purpose of this study, data set of seismic events recorded by the Frenštát seismic network (denoted as SPF; location of stations is on the Figure 1) during the period 1992 – 2002 was compiled. The SPF network was in operation 10 years with no interruption and no change of seismic instrumentation, so the recorded data are suitable for the purpose of this study, it means investigation of discrimination techniques to distinguish natural and mining induced seismic events. Epicenters of selected seismic events recorded during 10 years of monitoring at the stations of SPF cover area of 60 x 60 km and they are displayed on the map in Figure 1. Tectonic events are located mainly north-westerly and westerly of seismic network, only one event is located close to mining claim in the Czech part of USCB. Mining induced events are selected so that they cover all undermined areas in the Czech part of USCB (Ostrava sub-basin, Petřvald sub-basin, Karviná sub-basin, Starýč area).

The Czech part of the USCB is situated on the northeastern edge of the Czech Republic and geologically it belongs to the segment of Variscide orogeny. Upper Carboniferous strata represent hard rocks of basin including coal seams. Carboniferous formations are buried with Quaternary and Tertiary sedimentary rocks. The thickness of these sedimentary rocks is variable – from first meters to several hundreds of meters. The tectonic structure and stress conditions in USCB are described in detail in the papers [WPG13], [GW11], [PGKW12]. The territory of SPF seismic network is characterized by close contact between the Outer Carpathians and

| Code of station | Name             | Lon    | Lat    | h (m) |
|-----------------|------------------|--------|--------|-------|
| TRO             | Trojanovice      | 18.174 | 49.523 | 435   |
| PST             | Pstruží          | 18.326 | 49.575 | 461   |
| PAL             | Palkovické Hůrky | 18.273 | 49.640 | 517   |
| CEL             | Čeladná          | 18.333 | 49.520 | 454   |
| VYS             | Vyšní Lhoty      | 18.476 | 49.637 | 456   |

Table 1: The coordinates of the stations from SPF.

the Bohemian Massif. The margin of the Outer Carpathians overfault to the Miocene foredeep follows the southern margin of the Ostrava Quaternary basin (see [HJ04]).

### 3 SPF seismic network

The SPF seismic network consisted of 5 seismic stations located at the territory of  $20 \times 20$  km in the south part of the USCB. See Figure Coordinates and names of stations are presented in Table 1. Seismic stations were equipped with 3-component seismometers WDS-202 ( $f_0 = 2$  Hz) placed in a shallow boreholes at the depth approximately 30 m below the surface. Seismic signal was recorded by the apparatus PCM3-T in triggered regime after amplitude had reached trigger level at least at one station. The sampling frequency of recorded signal was 125 Hz. Recorded data from all stations were concentrated by the relay station situated at the top of the Beskydy mountains at a communication tower equipped with a data concentrator based on microcomputer SAPI-1. Afterwards data were transmitted by radio transmitter to the recording center in Ostrava. Recorded data files were converted into the ESTF/2 format, which was modified from the standard ESTF format by transferring 4 byte signal amplitude information into 2 byte form. It enabled reduction of recorded data volume by a half. Special seismic interpretation system WAVE was developed for recorded digital data processing with individual program packages enabling given analysis – localization, spectral analysis, polarization analysis, focal mechanism determination. Within this study, the software WAVE has been used for conversion of selected seismic signals from the ESTF/2 format to ASCII.

### 4 Seismological station Ostrava-Krásné Pole

The station Ostrava-Krásné Pole (OKC) —  $49.83460^\circ\text{N}$ ,  $18.13990^\circ\text{E}$ ,  $h = 250\text{m}$  — was established in 1983. It is operated by the Institute of Geonics of the Czech Academy of Science (CAS), the Institute of Geophysics of the CAS and the VŠB – Technical University of Ostrava. It is a part of the Czech regional seismic network as well as the international network of stations. It is equipped with three-component short-period SM3 sensors — suitable mainly for registering nearby induced seismic phenomena in the Upper Silesia Coal Basin — and the wide-band seismometer of the manufacturer Guralp for registering more distant earthquakes. The sensors are located in a shallow tunnel with a small seismic disturbance. The Quanterra Q330S registration apparatus is located in the building of the Astronomical Observatory of Johan Palisa. The station operates online and digital data (since 2007) are transferred in real time to the Institute of Geophysics. It mainly contributes to the rapid localization of mining-induced seismic events, local tectonic phenomena and major world earthquakes.

The station OKC is also part of a local seismic network that monitors the earthquakes associated with coal mining in the Upper Silesian Coal Basin (OKR, Poland) and natural seismicity in Northern Moravia and Silesia.

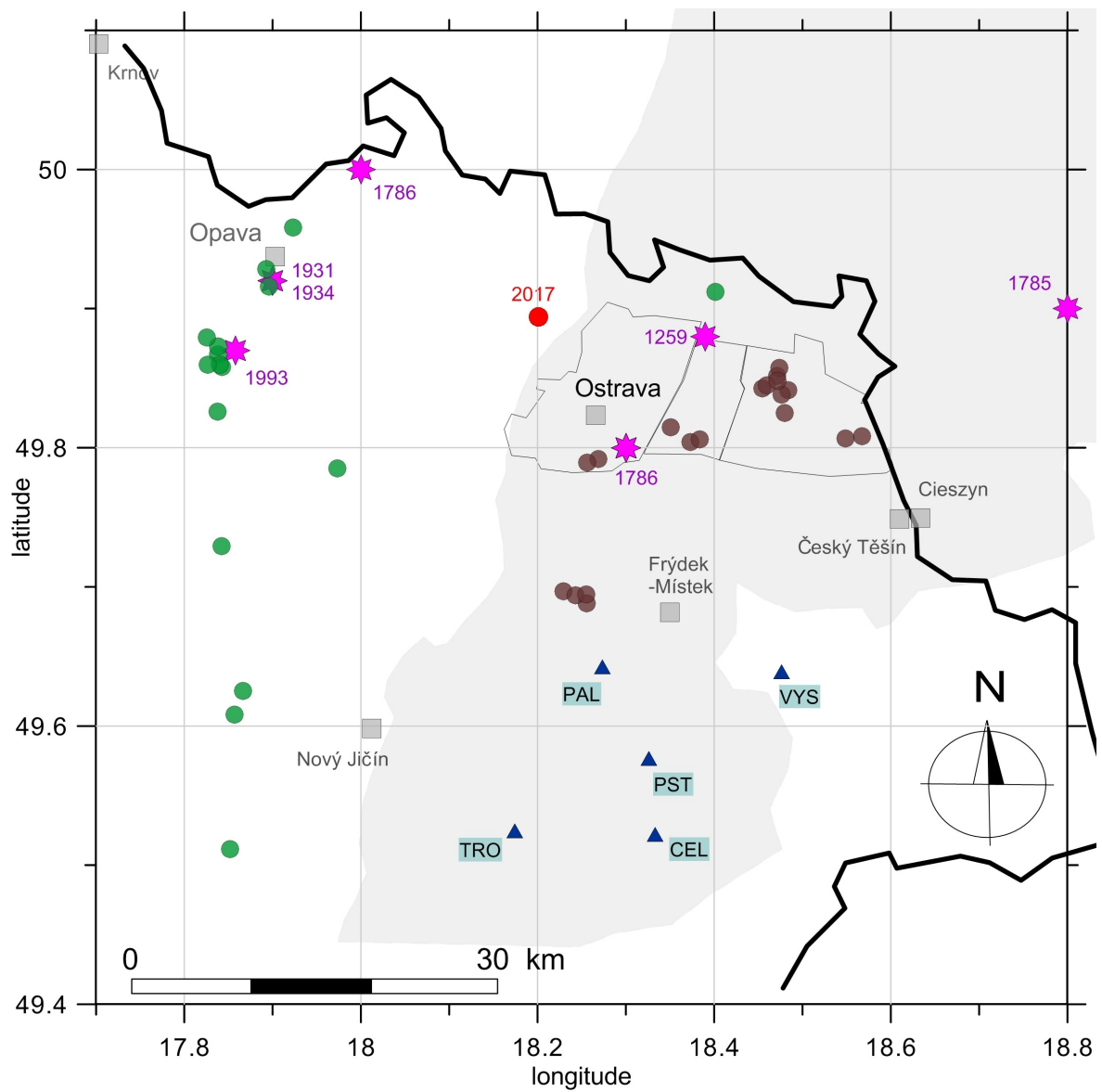


Figure 1: A map of the strongest earthquakes in the Northeastern region of the Czech Republic, the stations of the Seismic Polygon Frenštát (SPF), the Czech part of The Upper Silesian Coal Basin (light grey).

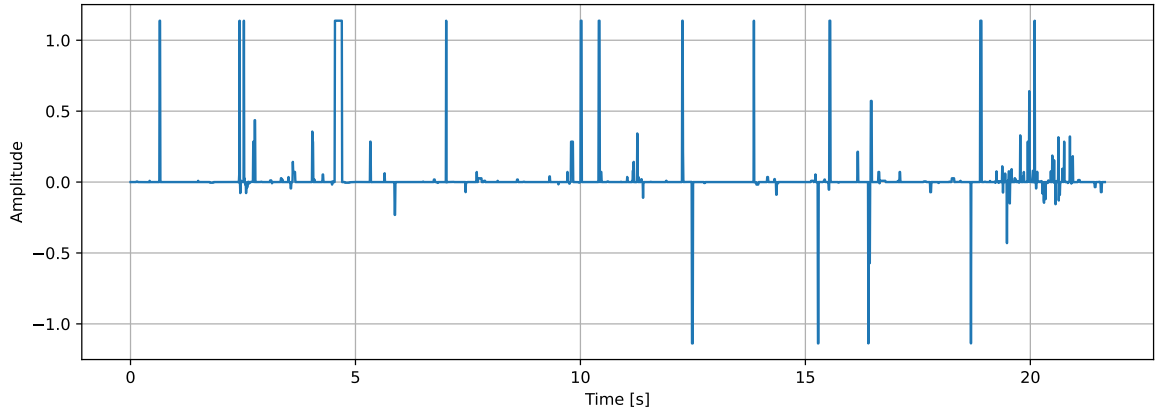


Figure 2: A clipped signal.

The main issue of the dataset produced by the station OKC (2007 – present) is lack of natural tectonic events for training a suitable machine learning model.

## 5 Seismic input data

Since there is not enough natural seismic events in the OKC dataset, we use the data from SPF, which captured the tectonic events occurred in 90s, providing a valuable dataset for training our model.

### 5.1 Data preparation

**Format conversion.** The data of SPF was originally stored in a custom ESTF/2 format. Therefore, we implemented a decoder to the SEED format which is a modern standard for exchange of earthquake data.

**Data cleaning.** As we described above, the analyzed data set consists of seismic signals recorded in a triggered regime at 5 stations of SPF network between the years 1992 – 2002. Although all seismic events were always recorded at all five stations, not all records were suitable for the analysis due to a bad quality of signal which could be distorted.

To detect corrupted or anomalous waveforms prior to further usage for ML models, we implemented a lightweight amplitude-based quality control procedure based on an observation of a particular corrupted data. The method operates directly in the time domain and applies three complementary heuristics to each channel of the seismic signal:

- Hard amplitude threshold.

Any sample reaching an absolute amplitude of the maximum value is considered invalid, indicating potential clipping of the signal. See 2

- Excessive high-amplitude fraction.

If more than 35 % of samples within a component exceed an absolute amplitude of  $0.8 \times$  the maximum value, the event is marked. This criterion targets records that are either heavily clipped or exhibit long periods of unrealistically high amplitude. See 3

- Global distribution imbalance.

For each component, the mean of the absolute amplitudes is computed. If at least 95 % of the samples fall below this mean, the distribution is deemed pathological, suggesting

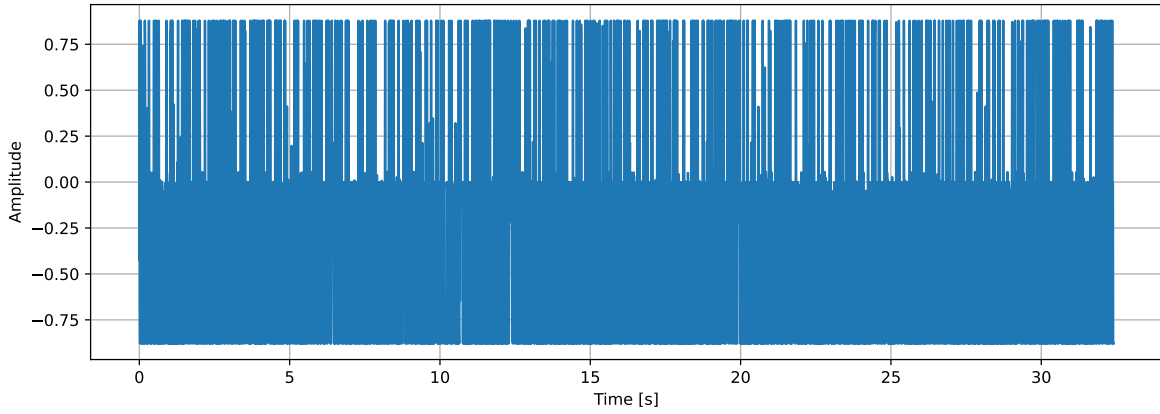


Figure 3: A distorted signal with high amplitude.

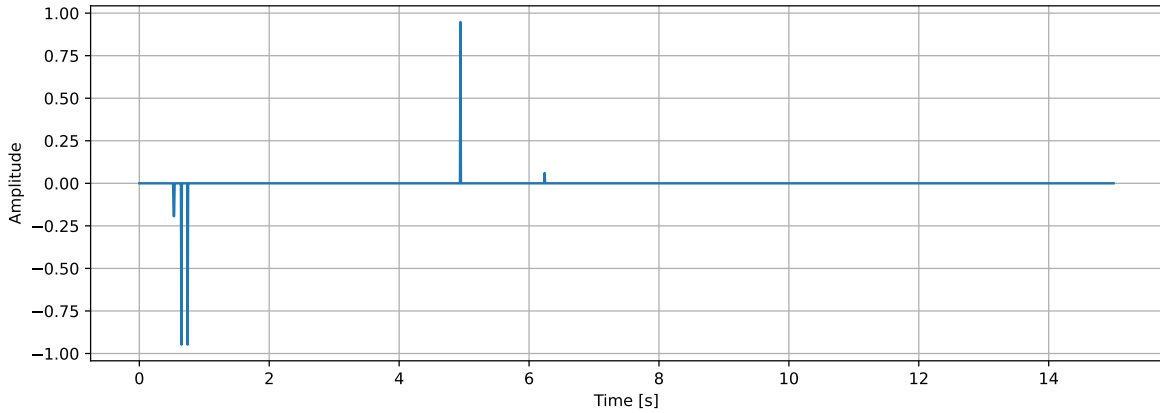


Figure 4: A very weak signal with several unrealistic ‘peaks’.

that the component is dominated by abnormally small values with a minority of large excursions. See Figure 4.

An event record is marked as corrupted if any its component waveform violates at least one of the above conditions. The data marked as corrupted were also visually checked. In total, we removed 14,133 records and for the further analysis we used 59,498 records of mining-induced seismic events and 10,632 natural tectonic events. For more details see Table 2.

## 5.2 Preprocessing

We use the following preprocessing techniques. See 5

| Event type     | Events | Records (Events $\times$ 5) | No. Corrupted records | Records used  |
|----------------|--------|-----------------------------|-----------------------|---------------|
| All            | 17,384 | 86,920                      | 14,133                | 72,787        |
| Tectonic       | 2,516  | 12,580                      | 1,9481                | <b>10,632</b> |
| Mining-induced | 14,144 | 70,720                      | 11,222                | <b>59,498</b> |
| Quarry blast   | 639    | 3,195                       | 0.8861                | 2,657         |
| Other          | 85     | 425                         | 85 (skipped)          | 0             |

Table 2: A summary of the number of events and the records removed.

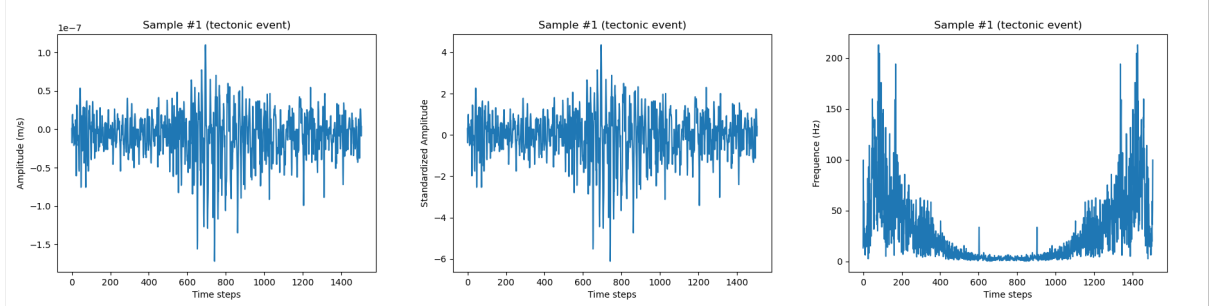


Figure 5: Raw seismic waveform in amplitude domain (left), standardized amplitude obtained (Z-Score; center), frequency domain obtained by FFT (right).

**Trimming.** For the machine model training, input time series (seismic events) must have the same length. This can be achieved by means of cutting events to the length of the shortest event.

**Z-Score.** A more suitable representation of events can be achieved using the Z-Score which is used to transform data into a standard normal distribution, ensuring that all features are on the same scale, which helps the model learn better.

**Fourier transform.** For better model performance we convert the signal from the time domain into the frequency domain using the Fast Fourier Transform algorithm (FFT). Note that when FFT is applied, trimming can be omitted.

## 6 Machine learning models

In this section, we briefly describe machine learning models we implemented and used for event classification. The models were implemented in the Python programming language using the PyTorch and the XGBoost frameworks.

### 6.1 Recurrent Neural network

First of all, we use the following types of recurrent neural networks.

#### 6.1.1 Long Short-Term Memory (LSTM)

LSTM networks (see [HS97]) are a type of recurrent neural network designed to capture long-range patterns while mitigating the vanishing gradient problem. We implemented a three-layer LSTM network with a hidden size of 64, dropout of 0.7, and input dimension of three for each channel of input seismic signal. The final hidden state is passed through a linear layer to predict two classes.

We use the AdamW solver for optimization and the Cross Entropy loss function in model training.

#### 6.1.2 Long Short Term Memory Fully Convolutional Network (LSTM-FCN)

To exploit both recurrent and convolutional feature extraction, we also tested the LSTM-FCN hybrid model (see [KMDC18]). The network consists of two branches, one with an LSTM block followed by a dropout layer. The second one consists of three 1D convolution layers followed

| Hyperparameter | Value |
|----------------|-------|
| Learning rate  | 0.001 |
| Batch size     | 64    |
| Epochs count   | 20    |

Table 3: Names and values of the hyperparameters used for the recurrent neural network training.

by a ReLU activation function, a batch normalization layer, and last layer is average global pooling. The output of two branches is concatenated and passed into the basic feedforward classification layer, followed by the softmax activation function.

Note that original LSTM-FCN works with univariate time series, i.e. time series with one feature per time step. To make LSTM-FCN compatible with the dataset used in the following benchmarks, events of which are multivariate time series, a dimension shuffle layer is added to branch with convolutions, and 1D convolution layers are replaced with 2D convolution layers that work with  $N \times 3$  matrix, where  $N$  is event length. LSTM-FCN used in our approach has a hidden size of the LSTM layer of 16, number of convolution channels is also 16.

As in the previous case, we use the AdamW solver and the Cross Entropy loss function.

## 6.2 Extreme Gradient Boosting (XGBoost)

For comparison with the neural network models, we also trained an XGboost classifier which is a scalable ensemble learning algorithm which is based on decision trees and uses gradient boosting. See [CG16].

The model used 1,000 boosting rounds with a maximum tree depth of 6, a learning rate of 0.05, subsampling and column subsampling rates of 0.8, and an L2 regularization term of 1.0. Class imbalance was treated by setting the scale\_pos\_weight parameter to the ratio of negative to positive samples in the training data. The implementation employed the histogram-based tree construction method (tree\_method="hist") with early stopping based on validation AUC.

## 7 Results

The data set used for training is divided into training and test sets in such a way that the test dataset contains 33 % of the original dataset events, and train dataset contains the rest of the dataset. Each model configuration is tested in 10 training attempts to observe possible outcomes of the training process. In addition, all configurations use the same train and test sets.

At the end of each epoch, the model is tested on the test set, and if performance is best among any other epoch, its parameters are selected as the best. Training attempt performance is the performance of the model with the best determined parameters in 30 epochs on the test dataset.

Each benchmark is supplemented with the highest F1-score among attempts.

For the recurrent neural network model training process we used the hyperparameters showed in Table 3.

### 7.1 Comparison of models

First, we compare the implemented models using the default parameter settings defined in Section 6. For this evaluation, we applied Z-score normalization and the Fast Fourier Transform

| Model    | Accuracy | Precision | Recall | F1-Score |
|----------|----------|-----------|--------|----------|
| LSTM     | 0.9788   | 0.9695    | 0.9470 | 0.9578   |
| LSTM-FCN | 0.9769   | 0.9678    | 0.9408 | 0.9537   |
| XGBoost  | 0.9900   | 0.8991    | 0.9833 | 0.9423   |

Table 4: A comparison of accuracy, precision, recall and F-1 score of the implemented models.

| Number of layers | hidden size | Accuracy      | Precision     | Recall        | F1-Score      |
|------------------|-------------|---------------|---------------|---------------|---------------|
| <b>3</b>         | <b>64</b>   | <b>0.9788</b> | <b>0.9695</b> | <b>0.9470</b> | <b>0.9578</b> |
| 3                | 32          | 0.9763        | 0.9666        | 0.9392        | 0.9523        |
| 3                | 16          | 0.9680        | 0.9464        | 0.9272        | 0.9365        |
| 6                | 16          | 0.9669        | 0.9567        | 0.9111        | 0.9321        |

Table 5: A comparison of different LSTM hyperparameter configurations. The default setting is shown in bold.

(FFT) as preprocessing steps, without trimming the data.

The results indicate that the models achieve comparable performance and that the two classes are well separable. The detailed metrics are reported in Table 4.

## 7.2 Evaluation of LSTM Hyperparameters

In this section, we analyze the impact of several key hyperparameters of the LSTM model. See Table 5. The benchmark was conducted using the same training and test sets as in the previous case, and the preprocessing steps remained unchanged. Namely, the Z-score normalization followed by the Fast Fourier Transform (FFT).

## 7.3 Influence of trimming and FFT in preprocessing

In the last section, we analyze the impact of the considered preprocessing techniques – specifically, trimming and the Fast Fourier Transform (FFT). The evaluation was performed on the LSTM model using its default parameter settings. See Table 6

## Acknowledgement.

This work was supported by the programme Dynamic Planet Earth of the Czech Academy of Sciences – Strategy AV21.

| Fourier transform used | Trimming used | Accuracy | Precision | Recall | F1-Score |
|------------------------|---------------|----------|-----------|--------|----------|
| Yes                    | No            | 0.9781   | 0.9651    | 0.9471 | 0.9558   |
| Yes                    | Yes           | 0.9135   | 0.8780    | 0.7576 | 0.8009   |
| No                     | Yes           | 0.9092   | 0.8861    | 0.7321 | 0.7814   |

Table 6: Impact of trimming and the Fast Fourier Transform (FFT) on the LSTM model performance.

## References

[CG16] Tianqi Chen and Carlos Guestrin. Xgboost: A scalable tree boosting system. In *Proceedings of the 22nd ACM SIGKDD international conference on knowledge discovery and data mining*, pages 785–794, 2016.

[D<sup>+</sup>97] Miroslav Dopita et al. *Geology of the Czech part of the Upper Silesian Basin*. Ministry of the Environment, Prague, 1997.

[GW11] Radomír Grygar and Petr Waclawik. Structural-tectonic conditions of Karviná Subbasin with regard to its position in the apical zone of Variscan accretion wedge. *Acta Montanistica Slovaca*, 16:159–175, 12 2011.

[HJ04] Karel Holub and Rušajová Jana. Induced seismic events in the Staríč and Paskov mine fields, Czech Republic. *Acta Montanistica Slovaca*, 9, 03 2004.

[HS97] Sepp Hochreiter and Jürgen Schmidhuber. Long short-term memory. *Neural Comput.*, 9(8):1735–1780, November 1997.

[KMDC18] Fazle Karim, Somshubra Majumdar, Houshang Darabi, and Shun Chen. LSTM fully convolutional networks for time series classification. *IEEE Access*, 6:1662–1669, 2018.

[PGKW12] Jiří Ptáček, Radomír Grygar, Petr Koníček, and Petr Waclawik. The impact of Outer Western Carpathian nappe tectonics on the recent stress-strain state in the Upper Silesian Coal Basin (Moravosilesian Zone, Bohemian Massif). *Geologica Carpathica*, 63:3–11, 02 2012.

[PP22] Ivan Prachař and Jana Pazdírková. Historical earthquake database for the Bohemian Massif. <https://doi.org/10.48790/HPAB-H834>, 2022. Interactive map / database.

[vZ18] Jan Šílený and Jan Zedník. Mechanism of the earthquake at Hlučín near Ostrava, Czech Republic, on December 10, 2017. *EGRSE – Exploration Geophysics, Remote Sensing and Environment*, XXV(1):83–91, 2018.

[WPG13] Petr Waclawik, Jiří Ptáček, and Radomír Grygar. Structural and stress analysis in mining practice in the Upper Silesian Coal Basin. *Acta Geodynamica et Geomaterialia*, 10:255–265, 11 2013.